Multichannel Blind Signal Separation and Reconstruction

Sanyogita Shamsunder and Georgios B. Giannakis, *Fellow, IEEE*

***Abstract*— Separation of multiple signals from their superposition recorded at several sensors is addressed. The methods employ polyspectra of the sensor data in order to extract the unknown signals and estimate the finite impulse response (FIR) coupling systems via a linear equation based algorithm. The procedure is useful for multichannel blind deconvolution of colored input signals with (possibly) overlapping spectra. An extension of the main algorithm, which can be applied for quasiperiodic signal separation, is also given. Simulation results corroborate the applicability of the algorithm.**

I. Introduction

SEPARATION of multiple signals from their superposition recorded at several sensors is an important problem that shows up in a variety of applications such as communications, biomedical and speech processing. The task is made difficult by the fact that very little is known about the transmission channel or the input signals and thus the separation is "blind." A special class of multichannel systems is one where the output signals are a superposition of the primary and secondary signals linearly coupled from the other unknown channels. For example, with more than one speaker present and several microphones, a particular microphone not only records the primary speaker but reflections from other speakers as well [20]. Due to background noise and interference, the performance of speech recognition systems severely degrades. While traditionally noise cancellation schemes using microphones have been proposed, these typically assume the availability of the "clean" interfering signal [21] and ignore the cross-channel interaction. Assuming that there are L microphones recording L speakers and cross talk, the signal recorded by the lth microphone is[1]

$$x_l(t) = s_l(t) + \sum_{i=1, i\neq l}^{L} \sum_{\tau=0}^{Q} h_{li}(\tau) s_i(t-\tau). \tag{1}$$

Manuscript received March 3, 1995; revised January 30, 1997. The work of G. B. Giannakis was supported by ONR Grant N00014-93-1-0485. This paper was presented in part at the Sixth Digital Signal Processing Workshop, Yosemite National Park, CA, October 3–5, 1994. The associate editor coordinating the review of this manuscript and approving it for publication was Prof. John H. L. Hansen.

S. Shamsunder is with the Department of Electrical Engineering, Colorado State University, Fort Collins, CO 80523 USA (e-mail: sanyo@lance.colostate.edu).

G. B. Giannakis is with the Department of Electrical Engineering, University of Virginia, Charlottesville, VA 22903 USA.

Publisher Item Identifier S 1063-6676(97)07846-2.

[1] Real channels are assumed throughout; however, the algorithms can be easily adapted to the complex channels encountered in communication problems.

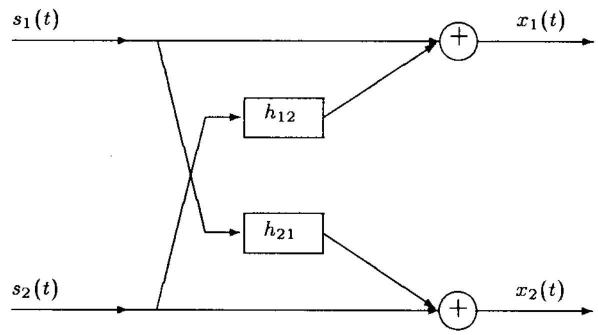

Fig. 1. Two-input, two-output signal model.

In (1), $s_l(t)$ is the signal recorded by the lth microphone in the absence of other inputs. The objective then is to separate the signals $s_l(t)$ from this superposition. In the vector form, (1) becomes

$$\mathbf{x}(t) = \sum_{\tau=0}^{Q} \mathbf{H}(\tau)\mathbf{s}(t-\tau) \tag{2}$$

where

$$\mathbf{H}(\tau) = \begin{bmatrix} 1 & h_{12}(\tau) & \dots & h_{1L}(\tau) \\ h_{21}(\tau) & 1 & \dots & h_{2L}(\tau) \\ \vdots & \vdots & \ddots & \vdots \\ h_{L1}(\tau) & h_{L2}(\tau) & \dots & 1 \end{bmatrix} \tag{3}$$

and $\mathbf{x}(t)$ [$\mathbf{s}(t)$] is the vector of observed [input] signals. For sake of simplicity, consider the two-channel system (results are presented in the sequel for the L-channel case). The observed signals can be written as (see Fig. 1)

$$x_1(t) = s_1(t) + \sum_{\tau=0}^{Q_1} h_{12}(\tau) s_2(t-\tau) \tag{4}$$

$$x_2(t) = s_2(t) + \sum_{\tau=0}^{Q_2} h_{21}(\tau) s_1(t-\tau) \tag{5}$$

and the objective is to estimate the coupling channel response $h_{li}(t)$ and separate the signals $s_l(t)$ given the 2×1 vector observations $\mathbf{x}(t), t = 0, 1, \cdots, T-1$. In the frequency domain, (2) can be expressed as

$$\mathbf{x}(\omega) = \mathbf{H}(\omega)\mathbf{s}(\omega) \tag{6}$$

where

$$\mathbf{H}(\omega) = \begin{bmatrix} 1 & H_{12}(\omega) \\ H_{21}(\omega) & 1 \end{bmatrix}$$

1063–6676/97$10.00

for the two-channel case. If $h_{li}(t)$ are known, $s_l(t)$ can be recovered via inverse (or Wiener) filtering.

The simplest multichannel signal separation problem with the channel coefficients assumed to be scale factors (i.e., a memoryless channel) has been extensively studied in the literature. In [4]–[8] and [16] linear and nonlinear methods for separation of independent signals from their superposition was addressed while multichannel autoregressive moving average (ARMA) identifiability results were given in [11] and [17]. In [18], the results of [4] were extended, and identifiability results were also given for input signals with memory while still restricting the channels to be memoryless (see also [19]). By imposing a parametric (ARMA) structure on the channel response, identification of multichannel systems with memory and independent, identically distributed (i.i.d.) inputs was studied in [17]. The present model of (6) is a generalization of those studied in the existing literature since it allows inputs *and* channels with memory (wideband case). Similar to the existing approaches, the inputs are assumed mutually (spatially) independent but not necessarily temporally independent; hence, colored inputs are also allowed.

The class of multichannel systems where the transfer matrix has the special structure of (3) was first considered in [20] and a decorrelation criterion was proposed for extracting signals from the observed mixtures. The analysis was carried out for the two-channel case, and it was pointed out that the criterion is insufficient for signal separation unless additional conditions hold, e.g., one of the coupling channels is known. Subsequently, in [22] a polyspectrum based method similar to that of [20] was suggested to broaden the class of identifiable systems without assuming knowledge of one of the channels. The algorithms in [20] and [22] are iterative, switch back and forth between the two channels and leave a shaping filter ambiguity in their recovered inputs. Convergence issues were not studied and extensions to more than two channels appears rather cumbersome. More recently in [12] a decorrelation criterion similar to [20] was applied for channel identification with AR inputs and MA coupling systems. In this case, the overall multi-input, multi-output can also be modeled as in [17].

Motivated by these limitations, in this paper we propose a fourth-order spectra based algorithm that is capable of uniquely estimating finite impulse response (FIR) channels. A computationally less intensive method which employs the bispectrum is proposed for minimum-phase channels. Although [22] and [18] (with memoryless transfer matrix) advocate speech enhancement applications, their derivations only deal with stationary processes and hence are applicable to unvoiced speech. The proposed algorithms on the other hand, are also applicable to a class of quasiperiodic signals and are thus particularly suitable for voiced as well as unvoiced speech enhancement.

While the paper concentrates on bispectrum and trispectrum based methods, the results can be generalized to kth-order spectra. The following assumptions are placed on the systems and the signals involved.

[A1] $s_l(t)$ are non-Gaussian, independent of each other and have nonzero kth-order spectra in the frequency band over which the channel responses are nonzero. Due to the nature of the signals involved no assumption is made regarding stationarity of $s_l(t)$ except that their statistics obey the following conditions (see also [10]):

[s1] All auto and cross-cumulants of $s_l(t)$, are absolutely summable[2], [10]

$$\sum_{\tau_1=-\infty}^{\infty} \cdots \sum_{\tau_{k-1}=-\infty}^{\infty} \sup_t |\tau_l \operatorname{cum}\{s_{l_0}(t), s_{l_2}(t+\tau_1), \ldots, s_{l_k}(t+\tau_{k-1})\}| < \infty, \tag{7}$$

for $l = 0, 1, 2, \ldots, L$ with $\tau_0 = 1$.

[s2] $\lim_{T\to\infty} \frac{1}{T} \sum_{t=0}^{T-1} E\{s_{l_0}(t) s_{l_1}(t+\tau_1) \ldots s_{l_{k-1}}(t+\tau_{k-1})\}$ exists.

[A2] The channels $H_{li}(\omega)$ are FIR of unknown order (Q in (1) is not known).

[A3] $\det[\mathbf{H}(\omega)] \neq 0 \ \forall\ \omega$.

The first assumption is standard and is equivalent to the persistence of excitation condition required by scalar system identification. If $s_l(t)$ are nonstationary, then conditions **[s1]** and **[s2]** are required so that sample kth-order (cross) moments of $x_l(t)$ converge to the appropriate limits (see the latter part of Section II for estimation of sample cumulants and polyspectra). Note that **[s2]** is satisfied both by stationary inputs as well as by quasi- or almost-periodic deterministic signals; hence, (un-)voiced speech satisfies **[s2]**. **[A2]** is needed for unique separation of signals; if the channels are not FIR, it will turn out that the inputs can be retrieved; however, a shaping filter ambiguity cannot be resolved (see also [22]). The third assumption is in reference to the invertibility of the multichannel system we alluded to after (6).

In Section II, the cumulants and polyspectra definitions used throughout the paper are presented, and the notation is established. The main results are described for the simpler case of a two-channel system in Section III, while Section IV is devoted to generalizing these algorithms to multichannel systems of size greater than two. Section V deals with input signal recovery via inverse filtering. The results are then specialized to cyclostationary signals, a subclass of nonstationary processes (Section VI). Experimental results with real and simulated data are presented in Section VII.

II. HOS of (Quasi-)Stationary Signals

In this section, we summarize the cumulant and polyspectra definitions for linear (quasi-)stationary processes. Higher order statistics, which are appropriate for stationary as well as nonstationary signals, will be defined via the time-averaged moments, cumulants and polyspectra. The reader is referred to [1, chap. 2] and [10] for further details and general definitions.

If two processes $x_l(t)$ and $x_m(t)$ are jointly stationary, zero-mean, and non-Gaussian, then their cross-cumulant used in this paper is

$$c_{(k-1)x_m x_l}(\boldsymbol{\tau}) \triangleq \operatorname{cum}\{x_m(t), x_m(t+\tau_1), \cdots, x_m(t+\tau_{k-2}), x_l(t+\tau_{k-1})\} \tag{8}$$

[2] In [10], $l = 0$ with $\tau_0 = 1$ was not included although it should be.

where $\boldsymbol{\tau} \triangleq (\tau_1, \tau_2, \cdots, \tau_{k-1})$ and the cumulant is defined in terms of the kth and lower order moments. The corresponding cross polyspectrum is denoted by $S_{(k-1)x_m x_l}(\boldsymbol{\omega})$, with $\boldsymbol{\omega} \triangleq (\omega_1, \cdots, \omega_{k-1})$.

Under **[A1]**, it can be shown using the multilinearity of cumulants [2, chap. 2] that the kth-order polyspectra of $x_l(t)$ in (1) is

$$S_{kx_l}(\boldsymbol{\omega}) = S_{ks_l}(\boldsymbol{\omega}) + \sum_{i=1, i\neq l}^{L} H_{li}^{(k)}(\boldsymbol{\omega}) S_{ks_i}(\boldsymbol{\omega}) \tag{9}$$

where $H_{li}^{(k)}(\boldsymbol{\omega}) \triangleq H_{li}(\omega_1) H_{li}(\omega_2) \cdots H_{li}(-\omega_1 - \omega_2 - \cdots - \omega_{k-1})$. Similarly, the cross-polyspectrum in general can be expressed as

$$\begin{aligned} S_{x_{l_0 \cdots l_{k-1}}}(\boldsymbol{\omega}) = \sum_{i=1}^{L} & H_{l_0 i}(-\omega_1 - \omega_2 - \cdots - \omega_{k-1}) H_{l_1 i}(\omega_1) \\ & \times H_{l_2 i}(\omega_2) \cdots H_{l_{(k-1)} i}(\omega_{k-1}) S_{ks_i}(\boldsymbol{\omega}). \end{aligned} \tag{10}$$

In particular, the cross-polyspectrum defined via the Fourier transform of (8) is obtained from (10) with $l_0 = l_1 = \cdots = l_{k-2} = l$ and $l_{k-1} = m$, $m \neq l$,

$$\begin{aligned} &S_{(k-1)x_l x_m}(\boldsymbol{\omega}) \\ &\quad = \sum_{i=1}^{L} H_{li}(\omega_1) H_{li}(\omega_2) \cdots H_{li}(\omega_{k-2}) H_{mi}(\omega_{k-1}) \\ &\quad\quad \times H_{li}(-\omega_1 - \omega_2 - \cdots - \omega_{k-1}) S_{ks_i}(\boldsymbol{\omega}). \end{aligned} \tag{11}$$

In practice, the sample estimators of the polyspectra and cumulants are employed. The polyspectra can be consistently estimated via periodogram or correlogram type estimators [2]. For example, the sample estimator for the kth-order (cross) moment of a zero-mean stationary processes $x_{l_i}(t)$ $0 \leq i \leq k-1$ based on T observations is

$$\begin{aligned} &\hat{m}_{x_{l_0 l_1 \cdots l_{k-1}}}(\tau_1, \tau_2, \ldots, \tau_{k-1}) \\ &\quad = \frac{1}{T} \sum_{t=0}^{T-1} x_{l_0}(t) x_{l_1}(t+\tau_1) \ldots x_{l_{k-1}}(t+\tau_{k-1}). \end{aligned} \tag{12}$$

The kth-order cumulant estimate can then be expressed in terms of the sample moments. The bispectrum estimated via the Fourier transform of the sample third-order cumulant is known as the *bicorrelogram*. Alternately, a smoothed version of the biperiodogram [2]

$$I_{x_{l_0 l_1 l_2}}(\omega_1, \omega_2) = \frac{1}{T} X_{l_0}(\omega_1) X_{l_1}(\omega_2) X_{l_2}(-\omega_1 - \omega_2) \tag{13}$$

may also be employed [fast Fourier transform (FFT) frequencies can be used in (13)]. The conditions required on the smoothing window are given in [2] and the resulting estimator $\hat{S}_{x_{l_0, l_1, l_2}}(\omega_1, \omega_2)$ is consistent. These definitions can be generalized to fourth-order and higher order spectra as well.

A. Cumulants and Polyspectra of Nonstationary Signals

If the input signals (and consequently the observations) are not stationary, the sample averages are inconsistent because of the ensemble averages being time-varying. Therefore, we will first define the time-averaged moment and cumulant that are appropriate for such signals. The kth-order time-averaged moment of a process $x(t)$ is

$$\begin{aligned} &\bar{m}_{kx}(\tau_1, \tau_2, \cdots, \tau_{k-1}) \\ &\quad \triangleq \lim_{T\to\infty} \frac{1}{T} \sum_{t=0}^{T-1} m_{kx}(t; \tau_1, \tau_2, \cdots, \tau_{k-1}). \end{aligned} \tag{14}$$

The time-averaged kth-order cumulant is expressed in terms of the moments of k and less. In particular, if $x(t)$ is zero-mean (in the time-averaged sense, i.e., (14) vanishes for $k=1$), then the time-averaged fourth-order cumulant is defined in terms of the time-averaged moments as

$$\begin{aligned} &\bar{c}_{4x}(\tau_1, \tau_2, \tau_3) \\ &\quad = \bar{m}_{4x}(\tau_1, \tau_2, \tau_3) - \bar{m}_{2x}(\tau_1)\bar{m}_{2x}(\tau_2 - \tau_3) - \bar{m}_{2x}(\tau_2) \\ &\quad\quad \times \bar{m}_{2x}(\tau_3 - \tau_1) - \bar{m}_{2x}(\tau_3)\bar{m}_{2x}(\tau_2 - \tau_1) \end{aligned} \tag{15}$$

with $\bar{m}_{4x}$ and $\bar{m}_{2x}$ given by (14) with $k = 4$, 2 respectively. The multilinearity property of conventional higher-than-second-order statistics also holds for time-averaged cumulants and polyspectra. The time-averaged polyspectra are the multidimensional Fourier transforms of the corresponding time-averaged cumulants and, thus, (9) and (11), hold with time-averaged polyspectra replacing the ensemble-based statistics.

In practice, the time-averaged cumulants and polyspectra can be estimated from sample averages if the signals $s_l(t)$ are jointly "quasistationary" in the sense of **[s1]** and **[s2]**. Under these conditions, the sample kth-order (cross) moments of $s_l(t)$, $l = 1, \cdots, L$ converge to the time averaged in the mean square sense [10]

$$\begin{aligned} &\lim_{T\to\infty} \frac{1}{T} \sum_{t=0}^{T-1} s_{l_0}(t) s_{l_1}(t+\tau_1) \ldots s_{l_{k-1}}(t+\tau_{k-1}) \\ &\quad \overset{\text{m.s.s}}{=} \lim_{T\to\infty} \frac{1}{T} \sum_{t=0}^{T-1} E\{s_{l_0}(t) s_{l_1}(t+\tau_1) \ldots s_{l_{k-1}}(t+\tau_{k-1})\}. \end{aligned} \tag{16}$$

Therefore, moments and, hence, cumulants and polyspectra can be consistently estimated using single data records. If the processes are stationary, then the expected value on the right-hand side of (16) is time invariant and thus validates the convergence of the sample averages for stationary processes.

Note that regardless of whether $s_l(t)$ are jointly stationary or nonstationary but satisfying **[s1]** and **[s2]**, in practice the sample estimator is the same. Also, since the input-output relations hold for ensemble as well as time averaged, we drop the overbar for the latter. We develop our algorithms based on the "true" polyspectra, keeping in mind that "true" refers to ensemble definitions for stationary signals and the time averaged for nonstationary processes. In Section VI, extensions of the proposed algorithm to cyclostationary signals will be studied, where we will define the appropriate cumulants and polyspectra.

III. Channel Estimation Based on Polyspectra

In order to recover the signals $s_l(t)$, we first need to estimate the channel impulse responses $h_{12}(t)$ and $h_{21}(t)$ so that the observed signals can be inverse filtered to obtain the interference-free signals. The frequency-domain approach described in this section provides a simple, linear solution to the channel estimation problem. This algorithm requires the knowledge of the "dc gain" $\mathbf{H}(\omega)|_{\omega=0}$ and hence we address this problem first in Section III-A.

A. Estimating $\mathbf{H}(0)$

The reconstruction algorithms to be developed in the subsequent sections assume that $H_i(0)$ is available. Note that unlike in the single-channel case, these quantities cannot be set arbitrarily for the unique extraction of the inputs. An eigendecomposition approach proposed in [4] and [18] for estimating a memory less multichannel matrix will be extended to the present scenario of estimating the transfer matrix entries at the dc frequency. The scheme proposed here is based on the spectrum and trispectrum of the channel outputs rather than on the fourth-order moments as in [4] and [18]. Thus, in addition to **[A1]** we need the following conditions on the input signal.

[A1′] The signal spectra are nonzero at the dc frequency, i.e., $S_{2s_l}(\omega)\mid_{\omega=0}\neq 0$, $\forall\, l$, and

$$\frac{S_{4s_k}(0,0,0)}{S_{2s_k}^2(0)} \neq \frac{S_{4s_l}(0,0,0)}{S_{2s_l}^2(0)} \neq 0, \quad k \neq l. \tag{17}$$

Note that **[A1′]** is less severe than the one imposed in [4] according to which all the input signals are not allowed to have identical kurtosis and resembles the time-domain assumption used in [18].

In multichannel identification, since second-order statistics provide a solution that is unique only up to a unitary matrix (an infinite set), see for e.g., [17], we combine the information provided by the trispectrum and the spectrum to yield a unique solution (a scale and shuffling ambiguity cannot be resolved [17], [19]). The spectral matrix of the observation vector $\mathbf{x}(t)$ in (2) is given by

$$\mathbf{S}_{2x}(\omega) = \lim_{T\to\infty}\frac{1}{T}E\{\mathbf{x}(\omega)\mathbf{x}^*(\omega)\} = \mathbf{H}(\omega)\mathbf{S}_{2s}(\omega)\mathbf{H}'(-\omega) \tag{18}$$

where the second equality follows from (6), $\mathbf{S}_{2s}(\omega)$ is the spectral matrix of the input signals, $\mathbf{H}(\omega)$ is the transfer function matrix, and * denotes the conjugate transpose. Under **[A1]** and **[A1′]**, let the eigendecomposition of the symmetric spectral matrix at $\omega = 0$ be

$$\mathbf{S}_{2x}(0) = \mathbf{H}(0)\mathbf{S}_{2s}(0)\mathbf{H}'(0) = \mathbf{U}\mathrm{diag}\{\lambda_1^2, \lambda_2^2, \cdots, \lambda_L^2\}\mathbf{U}' \tag{19}$$

where $\mathbf{U}$ is an orthogonal matrix consisting of the eigenvectors of $\mathbf{S}_{2x}(0)$. A transformation matrix $\mathbf{T} = \mathrm{diag}\{1/\lambda_1, 1/\lambda_2, \cdots, 1/\lambda_L\}\mathbf{U}^{-1} = \mathrm{diag}\{1/\lambda_1, \cdots, 1/\lambda_L\}\mathbf{U}'$, when applied to the output vector observations $\mathbf{x}(\omega)$ yields

$$\mathbf{y}(\omega) = \mathbf{T}\mathbf{x}(\omega) = \mathbf{T}\mathbf{H}(\omega)\mathbf{s}(\omega) = \mathbf{G}(\omega)\mathbf{s}(\omega). \tag{20}$$

Our goal is to identify $\mathbf{H}(0) = \mathbf{T}^{-1}\mathbf{G}(0)$ and since $\mathbf{T}$ is available from the eigendecomposition of $\mathbf{S}_{2x}(0)$, we focus next on recovering $\mathbf{G}(0)$.

It can be easily shown from (19) and the definition of $\mathbf{T}$ that $\mathbf{S}_{2y}(0)$ is an identity matrix

$$\mathbf{S}_{2y}(0) = \mathbf{T}\mathbf{S}_{2x}(0)\mathbf{T}' = \mathbf{T}\mathbf{H}(0)\mathbf{S}_{2s}(0)\mathbf{H}'(0)\mathbf{T}' = \mathbf{I} \tag{21}$$

which implies that $\mathbf{T}\mathbf{H}(0)\mathbf{S}_{2s}^{1/2}(0)$ is orthogonal. Since in our case, the inputs are mutually independent, the matrix $\mathbf{S}_{2s}(\omega)$ is diagonal and hence we conclude that the column vectors of $\mathbf{G}(0) \triangleq \mathbf{T}\mathbf{H}(0)$ are orthogonal with $\mathbf{G}'(0)\mathbf{G}(0) = \mathbf{S}_{2s}^{-1}(0)$ (see also [18]). If the ith column of $\mathbf{G}(\omega)$ is $\mathbf{g}_i(\omega)$ we have

$$\mathbf{g}_l'(0)\mathbf{g}_m(0) = \frac{1}{S_{2s_l}(0)}\delta(l-m) \tag{22}$$

where $S_{2s_l}(\omega)$ is the spectrum of $s_l(t)$. To recover $\mathbf{G}(0)$, we next appeal to the fourth-order (cross) spectrum of the transformed output $y_l(t)$ defined as

$$\begin{aligned} S_{4y_{mnkl}}(\omega_1,\omega_2,\omega_3) &= \sum_{\tau_1,\tau_2,\tau_3} \mathrm{cum}\{y_m(t), y_n(t+\tau_1),\ y_k(t+\tau_2), \\ &\quad y_l(t+\tau_3)\}e^{-j(\omega_1\tau_1+\omega_2\tau_2+\omega_3\tau_3)} \qquad (23)\\ &= \sum_{i=1}^{L} G_{mi}(-\omega_1-\omega_2-\omega_3)G_{ni}(\omega_1) \\ &\quad G_{ki}(\omega_2)G_{li}(\omega_3)S_{4s_i}(\omega_1,\omega_2,\omega_3) \qquad (24) \end{aligned}$$

where to obtain the last equality, we have used **[A1]** and (20), with $G_{kl}(\omega)$ denoting the (k,l) entry in the transformed matrix $\mathbf{G}(\omega)$.

The next step is to define a fourth-order spectral matrix and exploit (22) to simplify this matrix. With this in mind consider, the "averaged" trispectrum at $\omega_i = 0, i = 1, 2, 3$

$$\begin{aligned} S_{4y_{kl}}(0) &= \sum_{m=1}^{L} S_{4y_{mmkl}}(0,0,0) \qquad (25)\\ &= \sum_{i=1}^{L}\sum_{m=1}^{L} G_{mi}(0)G_{mi}(0)G_{ki}(0)G_{li}(0)S_{4s_i}(0,0,0) \qquad (26)\\ &= \sum_{i=1}^{L} \mathbf{g}_i'(0)\mathbf{g}_i(0)G_{ki}(0)G_{li}(0)S_{4s_i}(0,0,0) \qquad (27)\\ &= \sum_{i=1}^{L} \frac{S_{4s_i}(0,0,0)}{S_{2s_i}(0)}G_{ki}(0)G_{li}(0). \qquad (28) \end{aligned}$$

In arriving at (26), we used (24), and in obtaining the last equality we used (22). Collecting these trispectrum lags for

$k, l = 1, \cdots, L$ in a matrix, we obtain

$$\bar{\mathbf{S}}_{4y} = \sum_{i=1}^{L} \frac{S_{4s_i}(0,0,0)}{S_{2s_i}(0)} \mathbf{g}_i(0)\mathbf{g}_i'(0). \tag{29}$$

Under **[A1′]**, using (24), it follows that the columns of $\mathbf{G}(0)$ are given by the eigenvectors of $\bar{\mathbf{S}}_{4y}$ within a scale factor $S_{2s_l}(0)$ with the eigenvalues given by $S_{4s_l}/S_{2s_l}^2$ (recall that $\mathbf{g}_i(0)$ are orthogonal). On the other hand, if **[A1′]** does not hold, then there are multiple eigenvalues and, hence, the eigenvectors are non unique. After estimating $\mathbf{G}(0)$, the true matrix can be obtained[3] via $\mathbf{H}(0) = \mathbf{T}^{-1}\mathbf{G}(0)$.

It should be noted that since this procedure yields the columns of $\mathbf{G}(0)$, there is no unique way of assigning the eigenvectors to the columns of the transfer matrix. Further, each eigenvector also possesses a scaling ambiguity (since a scaled version of the "true" eigenvector is also an eigenvector). Thus, the matrix $\mathbf{G}(0)$ is obtained within a post multiplication by a permutation matrix (which shuffles the columns of $\mathbf{G}(0)$) and a diagonal matrix accounting for the unknown scale ambiguities associated with the eigenvectors (see [17] and [18] for proofs of related identifiability results). If the ratios $S_{4s_i}(0,0,0)/S_{2s_i}^2(0)$ are somehow known for the signals $s_i(t)$, then the permutation matrix and scale ambiguities can be resolved. In general however, if $\mathbf{H}(0)$ is a solution, so is $\tilde{\mathbf{H}}(0) = \mathbf{H}(0)\mathbf{P}\mathbf{\Lambda}$ where $\mathbf{P}$ is a permutation matrix consisting of exactly a single nonzero entry (which is one) in any row or column and $\mathbf{\Lambda}$ is a diagonal matrix [11], [17]. Note also that for a given L, there are $L!$ possible permutation matrices (thus, for a two-channel system, there are two permutation matrices, one with 1) one's along the main diagonal, and another with 2) one's along the antidiagonal).

At first sight it appears that this eigendecomposition approach can be repeated for all frequencies ω. However, the transfer matrix at each frequency can only be estimated within a permutation and diagonal matrix ambiguity (making the shuffling and scaling frequency dependent). Combining these individual matrices to get the impulse response matrix is an impossible task unless further information is available. Additionally, the computational load for singular value decomposition at each frequency can be very high. Therefore, we seek a simpler, linear equation based solution for estimating $\mathbf{H}(\omega)$, $\omega \neq 0$. An alternate method to deal with the shuffling is given in [3].

B. Channel Estimation Based on Trispectra

For the sake of simplicity and to be able to communicate the principle of the procedure, in this section we concentrate on the simple two-channel estimation problem that will be generalized to multiple channels in Section V.

Consider the auto- and cross-trispectral slices $S_{4x_1}(\omega_1, \omega_2, 0)$, and $S_{3x_1x_2}(\omega_1, \omega_2, 0)$, which under **[A1]** can be expressed as [c.f. (9), (11)]

$$\begin{bmatrix} S_{4x_1}(\omega_1,\omega_2,0) \\ S_{3x_1x_2}(\omega_1,\omega_2,0) \end{bmatrix} = \begin{bmatrix} 1 & H_{12}(0) \\ H_{21}(0) & 1 \end{bmatrix} \times \begin{bmatrix} S_{4s_1}(\omega_1,\omega_2,0) \\ H_{12}^{(3)}(\omega_1,\omega_2) S_{4s_2}(\omega_1,\omega_2,0) \end{bmatrix}. \tag{30}$$

Similarly, we also obtain another set of equations from the second channel

$$\begin{bmatrix} S_{3x_2x_1}(\omega_1,\omega_2,0) \\ S_{4x_2}(\omega_1,\omega_2,0) \end{bmatrix} = \begin{bmatrix} 1 & H_{12}(0) \\ H_{21}(0) & 1 \end{bmatrix} \times \begin{bmatrix} H_{21}^{(3)}(\omega_1,\omega_2) S_{4s_1}(\omega_1,\omega_2,0) \\ S_{4s_2}(\omega_1,\omega_2,0) \end{bmatrix}. \tag{31}$$

Now, since $\mathbf{H}(0)$ is known from Section III-A, under **[A3]**, the above equations can be solved to yield the input signal polyspectral slices as

$$S_{4s_1}(\omega_1,\omega_2,0) = \frac{S_{4x_1}(\omega_1,\omega_2,0) - H_{12}(0)S_{3x_1x_2}(\omega_1,\omega_2,0)}{1 - H_{21}(0)H_{12}(0)} \tag{32}$$

$$S_{4s_2}(\omega_1,\omega_2,0) = \frac{S_{4x_2}(\omega_1,\omega_2,0) - H_{12}(0)S_{3x_2x_1}(\omega_1,\omega_2,0)}{1 - H_{21}(0)H_{12}(0)}. \tag{33}$$

Therefore, assuming that $S_{4s_l}(\omega_1,\omega_2,0) \neq 0, \ \forall \ l$ in the frequency region (ω_1,ω_2) over which $H_l(\omega_1,\omega_2) \neq 0$ we obtain, from (30)–(33)

$$\begin{aligned} H_{21}^{(3)}(\omega_1,\omega_2) &= H_{21}(\omega_1)H_{21}(\omega_2)H_{21}(-\omega_1-\omega_2) \\ &= \frac{S_{3x_2x_1}(\omega_1,\omega_2,0) - H_{12}(0)S_{4x_2}(\omega_1,\omega_2,0)}{S_{4x_1}(\omega_1,\omega_2,0) - H_{12}(0)S_{3x_1x_2}(\omega_1,\omega_2,0)} \end{aligned} \tag{34}$$

$$\begin{aligned} H_{12}^{(3)}(\omega_1,\omega_2) &= H_{12}(\omega_1)H_{12}(\omega_2)H_{12}(-\omega_1-\omega_2) \\ &= \frac{S_{3x_1x_2}(\omega_1,\omega_2,0) - H_{21}(0)S_{4x_1}(\omega_1,\omega_2,0)}{S_{4x_2}(\omega_1,\omega_2,0) - H_{21}(0)S_{3x_2x_1}(\omega_1,\omega_2,0)}. \end{aligned} \tag{35}$$

From the bispectra in (34) and (35), the impulse responses can be estimated via any of the existing bispectrum based modeling schemes (see e.g., [13, chap. 10]). Notice that the problem now is reduced to reconstruction of a deterministic sequence $h_{lm}(t)$ from its bispectra. The approach of [14], which computes the magnitude and phase using the log bispectra, is particularly attractive when $h_{lm}(t)$ are FIR. The details of the algorithm are available in [14] and will not be repeated here. The steps for channel estimation from the sensor outputs $x_l(t)$, $l = 1, 2$, $t = 0, 1, \cdots, T-1$, are as follows.

Step 1: Compute the (cross) trispectra and spectra and estimate $\hat{\mathbf{H}}(0)$ via the algorithm of Section III-A.

Step 2: Compute the appropriate auto-and cross-trispectral slices of $x_1(t)$ and $x_2(t)$ and solve for the channel bispectra using $\hat{\mathbf{H}}(0)$, and (34) and (35) computed via the sample estimates of the output (cross) trispectra.

[3] A similar "joint diagonalization" approach using fourth-order cumulants was proposed in [5] for the blind estimation of memoryless matrix transformations.

Step 3: Employ the algorithm of [14] to estimate the impulse response $\hat{h}_{lm}(t)$ from the bispectra $\hat{H}^{(3)}_{lm}(\omega_1, \omega_2)$ estimated in [step 2].

With the estimates of $\mathbf{H}(t)$, the input signals can then be recovered via inverse (or if the signal-to-noise ratio is known, Wiener) filtering. This should be contrasted with the approach of [20], where one of the channels is assumed to be known and the other is estimated via the decorrelating criterion.

Alternately, if the system is not invertible (except at $\omega = 0$), the input signal trispectra can be recovered via (32) and (33). If $s_l(t)$ can be modeled as linear processes, (32) and (33) can be used for estimating the model parameters. This is particularly true in the present scenario where the inputs are typically speech signals that can be modeled as AR processes. The AR parameters can be estimated by employing trispectrum based identification algorithms [13, chap. 10] and can be directly used for compression, recognition or verification. In this case, the channel estimation step is bypassed and unnecessary computations are eliminated.

An important special case occurs for channels that have negligible or poor low frequency response. In this case, the frequency response matrix $H(\omega)$ at $\omega = 0$ is diagonal, and (32) and (33) are simplified. Thus, for identifying the cross-coupling in ac-coupled channels such as telephone user loops and microphones, the first step of estimating $H(\omega)|_{\omega=0}$ is skipped and the complexity of the procedure is considerably reduced.

C. Bispectrum-Based Methods for Minimum Phase Channels

The trispectrum-based method of Section III-B yields the bispectrum of the channel and, thus, allows nonminimum phase channels. If however, the system is minimum phase and the input signals have nonvanishing bispectra, then computational gains maybe achieved by employing the bispectrum instead of the trispectrum. Even with minimum phase channels as shown in [20] and [22], the correlation-based method does not yield the right solution when the inputs are colored (i.e., exhibit temporal dependence). If the input is colored, one can also model it as the output of a linear process with transfer function $H_{\text{IN}}(\omega)$ which can then be combined with the channel transfer function. The second-order statistics can then be used to model the minimum phase channel. However, this is not an option when the inputs are nonlinear processes. Further, it introduces unwanted parameters into the estimation procedure and the question of separating $H_{\text{IN}}(\omega)$ from the channel response $H_{\text{CH}}(\omega)$ is unresolved unless one imposes additional conditions on these transfer functions, e.g., $H_{\text{IN}}(\omega)$ is AR and $H_{\text{CH}}(\omega)$ is MA [12]. Motivated by these shortcomings, we explore a bispectrum-based scheme that does not pose these problems, and is appropriate for minimum-phase channel estimation.

Following steps similar to those in (32)–(35), we obtain using $S_{3x_m}(\omega, 0)$ and $S_{2x_m x_n}(\omega, 0)$, $m, n = 1, 2$, the channel spectra

$$H_{21}(\omega)H_{21}(-\omega) = \frac{S_{2x_2x_1}(\omega,0) - H_{12}(0)S_{3x_2}(\omega,0)}{S_{3x_1}(\omega,0) - H_{12}(0)S_{2x_1x_2}(\omega,0)} \tag{36}$$

$$H_{12}(\omega)H_{12}(-\omega) = \frac{S_{2x_1x_2}(\omega,0) - H_{21}(0)S_{3x_1}(\omega,0)}{S_{3x_2}(\omega,0) - H_{21}(0)S_{2x_2x_1}(\omega,0)}. \tag{37}$$

The channel impulse response can then be estimated by employing the well-established spectrum modeling techniques (see e.g., [13]). The input signal bispectral slices can also be found as in (32) and (33) with the (cross-) bispectra of $x_l(t)$ replacing trispectra. This information can be used for model identification via the bispectrum if the transfer matrix is not invertible. At the expense of identifiability, computational gains can be achieved via the bispectral approach. Note that the algorithm of [20] cannot uniquely estimate the channels even if they are minimum phase.

Both the algorithms assume that either the bispectrum or the trispectrum of the input signals are nonzero over the frequency band coinciding with that of the system responses. This condition on the polyspectra is equivalent to the persistence of excitation condition required for system identification methods. For processes with nonskewed probability density functins (pdfs), the bispectrum (and odd-ordered spectra) vanishes, the trispectrum, which is nonvanishing for most non-Gaussian processes, can be employed; this is especially true for most communication signals.

IV. Input Signal Reconstruction

Let us next examine the effect of the permutation and scaling ambiguity on the estimation of the channels for a 2×2 system. From (30) and (31), we define the vectors $\tilde{\mathbf{v}}_1(\omega_1, \omega_2)$ and $\tilde{\mathbf{v}}_2(\omega_1, \omega_2)$ as

$$\tilde{\mathbf{v}}_1(\omega_1,\omega_2) = \tilde{\mathbf{H}}^{-1}(0)\begin{bmatrix} S_{4x_1}(\omega_1,\omega_2,0) \\ S_{3x_1x_2}(\omega_1,\omega_2,0)\end{bmatrix} \tag{38}$$

$$\tilde{\mathbf{v}}_2(\omega_1,\omega_2) = \tilde{\mathbf{H}}^{-1}(0)\begin{bmatrix} S_{3x_2x_1}(\omega_1,\omega_2,0) \\ S_{4x_2}(\omega_1,\omega_2,0)\end{bmatrix} \tag{39}$$

where $\tilde{\mathbf{H}}(0)$ is the matrix obtained via the algorithm of Section III-A. Since a permutation and scaling matrix ambiguity is included, we have that $\tilde{\mathbf{H}}(0) = \mathbf{H}(0)\mathbf{P}\mathbf{\Lambda}$ (if $\mathbf{P}\mathbf{\Lambda} = \mathbf{I}$, then $\tilde{\mathbf{H}}(0) = \mathbf{H}(0)$). Therefore

$$\begin{aligned}\tilde{\mathbf{v}}_1(\omega_1,\omega_2) &\triangleq \mathbf{\Lambda}^{-1}\mathbf{P}^{-1}\mathbf{H}^{-1}(0)\begin{bmatrix} S_{4x_1}(\omega_1,\omega_2,0) \\ S_{3x_1x_2}(\omega_1,\omega_2,0)\end{bmatrix} \\ &= \mathbf{\Lambda}^{-1}\mathbf{P}^{-1}\begin{bmatrix} S_{4s_1}(\omega_1,\omega_2,0) \\ H^{(3)}_{12}(\omega_1,\omega_2)S_{4s_2}(\omega_1,\omega_2,0)\end{bmatrix} \\ &= \mathbf{\Lambda}^{-1}\mathbf{P}^{-1}\mathbf{v}_1(\omega_1,\omega_2)\end{aligned} \tag{40}$$

$$\begin{aligned}\tilde{\mathbf{v}}_2(\omega_1,\omega_2) &= \mathbf{\Lambda}^{-1}\mathbf{P}^{-1}\mathbf{H}^{-1}(0)\begin{bmatrix} S_{3x_2x_1}(\omega_1,\omega_2,0) \\ S_{4x_2}(\omega_1,\omega_2,0)\end{bmatrix} \\ &= \mathbf{\Lambda}^{-1}\mathbf{P}^{-1}\begin{bmatrix} H^{(3)}_{21}(\omega_1,\omega_2)S_{4s_1}(\omega_1,\omega_2,0) \\ S_{4s_2}(\omega_1,\omega_2,0)\end{bmatrix} \\ &= \mathbf{\Lambda}^{-1}\mathbf{P}^{-1}\mathbf{v}_2(\omega_1,\omega_2)\end{aligned} \tag{41}$$

where $\mathbf{P}^{-1}$ is also a permutation matrix and $\mathbf{\Lambda}^{-1}$ is a diagonal matrix. The vectors $\mathbf{v}_1(\omega_1, \omega_2)$ and $\mathbf{v}_2(\omega_1, \omega_2)$ are defined as in (38) and (39) but with the true $\mathbf{H}(0)$ (with no ambiguities). Thus, depending on the ambiguity in the estimation of $\mathbf{H}(0)$, we either obtain the true vector $\mathbf{v}_i(\omega_1, \omega_2)$ or the vector

$\tilde{\mathbf{v}}_i(\omega_1, \omega_2)$ that has its entries interchanged and scaled when compared to $\mathbf{v}_i(\omega_1, \omega_2)$.

We reiterate that for a 2×2 system, there are two choices for the permutation matrix $\mathbf{P}$, 1) with one's along the diagonal, or 2) with one's along the antidiagonal. If $\mathbf{P}^{-1}$ has ones along the antidiagonal, the first element in $\tilde{\mathbf{v}}_1(\omega_1, \omega_2)$ is $\lambda_1^{-1} H_{12}^{(3)}(\omega_1, \omega_2) S_{4s_2}(\omega_1, \omega_2, 0)$ while in $\tilde{\mathbf{v}}_2(\omega_1, \omega_2)$ it is $\lambda_1^{-1} S_{4s_2}(\omega_1, \omega_2, 0)$, where λ_i are the elements of $\mathbf{\Lambda}$. If the first (second) element in $\tilde{\mathbf{v}}_1(\omega_1, \omega_2)$ ($\tilde{\mathbf{v}}_2(\omega_1, \omega_2)$) is the "reference" for channel 1 (channel 2), then we obtain

$$\tilde{H}_{21}^{(3)}(\omega_1, \omega_2) = \frac{1}{H_{12}^{(3)}(\omega_1, \omega_2)} \tag{42}$$

$$\tilde{H}_{12}^{(3)}(\omega_1, \omega_2) = \frac{1}{H_{21}^{(3)}(\omega_1, \omega_2)}. \tag{43}$$

Therefore, in the situation where $\mathbf{P}^{-1}$ has ones along the antidiagonal, the ambiguity in estimating $\tilde{\mathbf{H}}(0)$ is nontrivial, and the channel frequency responses are[4]

$$\tilde{H}_{21}(\omega) = \frac{1}{H_{12}(\omega)}, \quad \tilde{H}_{12}(\omega) = \frac{1}{H_{21}(\omega)}. \tag{44}$$

If $\mathbf{P}$ is the trivial permutation matrix with ones along the diagonal, the channel responses are then

$$\tilde{H}_{21}(\omega) = H_{21}(\omega), \quad \tilde{H}_{12}(\omega) = H_{12}(\omega). \tag{45}$$

As a result, the overall transfer matrix $\mathbf{F}(\omega) = \tilde{\mathbf{H}}^{-1}(\omega)\mathbf{H}(\omega)$ is

$$\mathbf{F}(\omega) = \begin{bmatrix} 1 & 0 \\ 0 & 1 \end{bmatrix}, \text{ or, } \mathbf{F}(\omega) = \begin{bmatrix} 0 & H_{12}(\omega) \\ H_{21}(\omega) & 0 \end{bmatrix}. \tag{46}$$

If signal separation is all that is required (without regard to the actual signal) and a shaping filter ambiguity is tolerable, then either of the solutions is acceptable. However, if the channels are known to be FIR, then the solution in (44) is unacceptable and should be eliminated. The same considerations apply if the bispectrum-based algorithm of Section III-C is employed for estimating $\mathbf{H}(\omega)$. Consequently, unique estimation of the channels is feasible if

- **[r1]** the channels are FIR as per [**A2**], or
- **[r2]** the trispectrum and the spectrum at $\omega_i = 0$ is known for at least one of the input signals so that the estimation of $\mathbf{H}(0)$ does not introduce any shuffling ambiguities.

If a linear filter ambiguity can be tolerated in the extracted signals, then the above restrictions need not hold. This result coincides with that of [22]. However, the advantage of the proposed method is its simplicity when the channels are FIR. The frequency-domain approach is efficient with respect to implementation. The algorithm of [22] is iterative, and its convergence issues have not been studied. This is not the case with the proposed linear algorithm, which yields the correct solution under **[r1]** or **[r2]**, and the solution within a linear transformation in all other cases.

[4] Note that the scale factor cancels in the channel (bi)spectral estimation procedure and is thus inconsequential in the channel and input recovery.

V. Generalization to More than Two Channels

We now extend the results to the L-input, L-output scenario for the model of (1). When there are L channels, the $L \times 1$ vector of (cross-) polyspectra of all possible channel combinations is needed to generate enough equations to solve for the unknowns. Assuming as in (1) that $H_{ll}(\omega) = 1$, the vector with elements the auto- and cross-trispectra between the outputs $x_l(t)$ and $x_m(t)$ $m = 1, 2, \cdots, L$ is

$$\begin{bmatrix} S_{3x_lx_1}(\omega_1, \omega_2, 0) \\ S_{3x_lx_2}(\omega_1, \omega_2, 0) \\ \vdots \\ S_{3x_lx_l}(\omega_1, \omega_2, 0) \\ \vdots \\ S_{3x_lx_L}(\omega_1, \omega_2, 0) \end{bmatrix} = \mathbf{H}(0) \begin{bmatrix} H_{l1}^{(3)}(\omega_1, \omega_2) S_{4s_1}(\omega_1, \omega_2, 0) \\ H_{l2}^{(3)}(\omega_1, \omega_2) S_{4s_2}(\omega_1, \omega_2, 0) \\ \vdots \\ S_{4s_l}(\omega_1, \omega_2, 0) \\ \vdots \\ H_{lL}^{(3)}(\omega_1, \omega_2) S_{4s_L}(\omega_1, \omega_2, 0) \end{bmatrix}. \tag{47}$$

Again, let the matrix computed via the algorithm of Section III-A be $\tilde{\mathbf{H}}(0) = \mathbf{H}(0)\mathbf{P}\mathbf{\Lambda}$. With $\tilde{\mathbf{H}}(0)$ having a permutation ambiguity, the same considerations as in Section IV apply. From (47), we have as in (40) and (41)

$$\begin{aligned} \tilde{\mathbf{v}}_l(\omega_1, \omega_2) &= \mathbf{\Lambda}^{-1}\mathbf{P}^{-1}\mathbf{H}^{-1}(0) \begin{bmatrix} S_{3x_lx_1}(\omega_1, \omega_2, 0) \\ S_{3x_lx_2}(\omega_1, \omega_2, 0) \\ \vdots \\ S_{3x_lx_l}(\omega_1, \omega_2, 0) \\ \vdots \\ S_{3x_lx_L}(\omega_1, \omega_2, 0) \end{bmatrix} \\ &= \mathbf{\Lambda}^{-1}\mathbf{P}^{-1} \begin{bmatrix} H_{l1}^{(3)}(\omega_1, \omega_2) S_{4s_1}(\omega_1, \omega_2, 0) \\ H_{l2}^{(3)}(\omega_1, \omega_2) S_{4s_2}(\omega_1, \omega_2, 0) \\ \vdots \\ S_{4s_l}(\omega_1, \omega_2, 0) \\ \vdots \\ H_{lL}^{(3)}(\omega_1, \omega_2) S_{4s_L}(\omega_1, \omega_2, 0) \end{bmatrix} \\ &= \mathbf{\Lambda}^{-1}\mathbf{P}^{-1}\mathbf{v}_l(\omega_1, \omega_2). \end{aligned} \tag{48}$$

Thus, the vector $\tilde{\mathbf{v}}_l(\omega_1, \omega_2)$ is a permuted version of the "true" vector $\mathbf{v}_l(\omega_1, \omega_2)$ on the right-hand side of (48). Since the same permutation and diagonal matrix premultiplies all the vectors, the same swapping and scaling takes place in all $\tilde{\mathbf{v}}_l(\omega_1, \omega_2)$, $l = 1, \cdots, L$. Let us assume that due to the shuffling, the qth element in $\mathbf{v}_p(\omega_1, \omega_2)$ has moved to the pth location in $\tilde{\mathbf{v}}_p(\omega_1, \omega_2)$. The pth element in $\tilde{\mathbf{v}}_p(\omega_1, \omega_2)$ is now $H_{pq}^{(3)}(\omega_1, \omega_2) S_{4s_q}(\omega_1, \omega_2, 0)$ instead of $S_{4s_p}(\omega_1, \omega_2, 0)$ (the reference element). Due to similar shuffling in the remaining $L - 1$ vectors, the pth element in $\tilde{\mathbf{v}}_l(\omega_1, \omega_2)$ is $H_{lq}^{(3)}(\omega_1, \omega_2) S_{4s_q}(\omega_1, \omega_2, 0)$ instead of $H_{lp}^{(3)}(\omega_1, \omega_2) S_{4s_p}(\omega_1, \omega_2, 0)$, $l = 1, 2, \cdots, L$. Recalling that $H_{ll}^{(3)}(\omega_1, \omega_2) = 1$ and if because of the shuffle, we choose $H_{pq}^{(3)}(\omega_1, \omega_2) S_{4s_q}(\omega_1, \omega_2, 0)$ as the reference in the $\tilde{\mathbf{v}}_p(\omega_1, \omega_2)$, then

$$\tilde{H}_{lp}^{(3)}(\omega_1, \omega_2) = \frac{p\text{th element in } \tilde{\mathbf{v}}_l(\omega_1, \omega_2)}{p\text{th element in } \tilde{\mathbf{v}}_p(\omega_1, \omega_2)}$$

$$= \frac{H_{lq}^{(3)}(\omega_1,\omega_2)S_{4s_q}(\omega_1,\omega_2,0)}{H_{pq}^{(3)}(\omega_1,\omega_2)S_{4s_q}(\omega_1,\omega_2,0)}, \quad l=1,\cdots,L. \quad (49)$$

Thus, the corresponding channel response $\tilde{H}_{lp}(\omega)$ consists of poles and zeros. If we restrict ourselves to FIR channels (with $h_{1l}(t)$ having no zeros in common with $h_{kl}(t)$, $k=2,\cdots,L$, $\forall\, l$), this solution should be eliminated. For the "right" l, i.e., $l=q$, since $H_{qq}(\omega)=1$, $\tilde{H}_{lq}^{(3)}(\omega_1,\omega_2)$ in (49) will consist of poles only. If $l\neq p$, we conclude that a shuffle has taken place. This procedure can be repeated for $l=1,\cdots,L$ to infer if the corresponding columns of $\mathbf{H}(0)$ have been interchanged and estimate the permutation matrix. Note that as before, the scale factors are not of any consequence since $\tilde{H}_{kl}^{(3)}(\omega_1,\omega_2)$ in (49) is expressed as a ratio, with the same scale factors in the numerator and denominator. Again, if a shaping filter ambiguity can be tolerated, the above procedure need not be carried out and the FIR assumption on the channels is not needed.

VI. Extensions to Cyclostationary Signals

It is quite possible that, for some signals, the polyspectra do not satisfy the conditions in **[A1]** and **[A1′]**. The sinusoidal model for speech suggests that especially voiced speech exhibit (quasi-)periodicity and hence falls into the class of (almost) cyclostationary signals. This property can be exploited to further relax **[A1]** and **[A1′]**. In this section, extension of the preceding algorithms to cyclostationary signals is outlined.

Processes with periodically time-varying statistics are known as *cyclostationary signals* in the signal processing literature (see, e.g., [9]). If $y(t)$ is kth-order cyclostationary, then the time-varying cumulant $c_{ky}(t;\boldsymbol{\tau})$ is (almost) periodic. The cyclic cumulants are the generalized Fourier series coefficients of the time-varying cumulants. The cyclic cumulant at cycle α is[5]

$$\mathcal{C}_{ky}(\alpha;\boldsymbol{\tau}) = \lim_{T\to\infty}\frac{1}{T}\sum_{t=0}^{T-1} c_{ky}(t;\boldsymbol{\tau})e^{-j\alpha t}. \quad (50)$$

The cyclic polyspectrum is the Fourier transform of the cyclic cumulant defined as

$$\mathcal{S}_{ky}(\alpha;\boldsymbol{\omega}) = \sum_{\boldsymbol{\tau}} \mathcal{C}_{ky}(\alpha;\boldsymbol{\tau})e^{-j\sum_{l=1}^{k-1}\tau_l\omega_l}. \quad (51)$$

If $y(t)$ is stationary, then its cyclic cumulant and polyspectrum are nonzero only for $\alpha=0$.

It has been shown that the cyclic cumulants and polyspectra can be estimated consistently using a single set of observations if the process $y(t)$ satisfies some mild conditions [9]. The sample third-order cyclic cumulant estimator for the zero-mean $y(t)$ is given by

$$\hat{\mathcal{C}}_{3y}(\alpha;\tau_1,\tau_2) = \frac{1}{T}\sum_{t=0}^{T-1} y(t)y(t+\tau_1)y(t+\tau_2)e^{-j\alpha t}. \quad (52)$$

[5] For $\alpha=0$, the cyclic moment reduces to the time-averaged moment in (14).

The fourth-order cyclic cumulant estimator is defined in terms of the fourth- and second-order cyclic moments for a zero-mean process.

A useful property of the cyclic cumulants and polyspectra is that if two signals do not share the same cycle frequency, they can be separated in the cyclic domain; the multilinearity property of the conventional higher order statistics holds for cyclic cumulants as well. If the signals are cyclostationary and the channels are time invariant, we can employ the cyclic polyspectra instead of the conventional polyspectra in the channel estimation procedure described hitherto. Note that the spectrum cycle frequencies are in general different from the cycle frequencies present in the trispectrum. We denote the cycle frequency shared by the kth-order spectrum of all the input signals $s_l(t)$ with α_k.

In this section, we replace assumptions **[A1]** and **[A1′]** with the following ones to include cyclostationary processes.

- **[C1]** $s_l(t)$, $l=1,\cdots,L$ are zero-mean, non-Gaussian, cyclostationary, and mutually independent. The cyclic polyspectra $\mathcal{S}_{ks_l}(\alpha;\boldsymbol{\omega})\neq 0$ for at least one $\alpha=\alpha_k$ and $\forall\boldsymbol{\omega}$ in the frequency range over which $H_l(\omega)\neq 0$.
- **[C1′]** The cyclic spectrum $\mathcal{S}_{2s_l}(\alpha;0)\neq 0$, for at least one cycle $\alpha=\alpha_2$, $\forall\, l$. Additionally

$$\frac{S_{4s_k}(\alpha_4;0,0,0)}{S_{2s_k}^2(\alpha_2;0)} \neq \frac{S_{4s_l}(\alpha_4;0,0,0)}{S_{2s_l}^2(\alpha_2;0)} \neq 0, \quad k\neq l. \quad (53)$$

Consider again the signal model in (1) under [**C1**]. Observe from (50) and (51) that the cyclic higher order statistics have the same form as the conventional cumulants and polyspectra. Since the multilinearity property holds for cyclic cumulants as well, and since all the input signals cumulants/polyspectra share the same cycle frequency α_k as in (9) and (11), we conclude that the auto- and cross-cyclic polyspectra of $x_l(t)$ and $x_m(t)$ are given (see for e.g., [9]) by

$$S_{kx_l}(\alpha_k;\boldsymbol{\omega}) = S_{ks_l}(\alpha_k;\boldsymbol{\omega}) + \sum_{i=1,i\neq l}^{L} H_{li}^{(k)}(\boldsymbol{\omega})S_{ks_i}(\alpha_k;\boldsymbol{\omega}) \quad (54)$$

$$\begin{aligned} S_{(k-1)x_lx_m}&(\alpha;\boldsymbol{\omega}) \\ &= \sum_{i=1}^{L} H_{li}(\omega_1)H_{li}(\omega_2)\ldots H_{li}(\omega_{k-2})H_{mi}(\omega_{k-1}) \\ &\quad \times H_{li}(-\omega_1-\omega_2-\cdots-\omega_{k-1})S_{ks_i}(\alpha_k;\boldsymbol{\omega}). \end{aligned} \quad (55)$$

For $\alpha=0$, we get the polyspectra for stationary signals [see (9) and (11)]. By employing now the cyclic trispectra (bispectra) in the algorithms of Section III and III-C, the channel bispectra [spectra], $H_{kl}^{(3)}(\omega_1,\omega_2)$ [$H_{kl}^{(2)}(\omega)$], can be obtained. The remaining procedure for estimating the impulse response is the same as before provided **[C1′]** holds. For estimating $\mathbf{H}(0)$, we use the cyclic spectral matrix with entries $\mathcal{S}_{x_lx_m}(\alpha_2;0)$ and the cyclic trispectrum $\mathcal{S}_{4y_{iikl}}(\alpha_4;0,0,0)$ in (19) and (25), respectively. As long as all the input signals share the same cycles in their spectra and trispectra, the procedure of Section III-A applies.

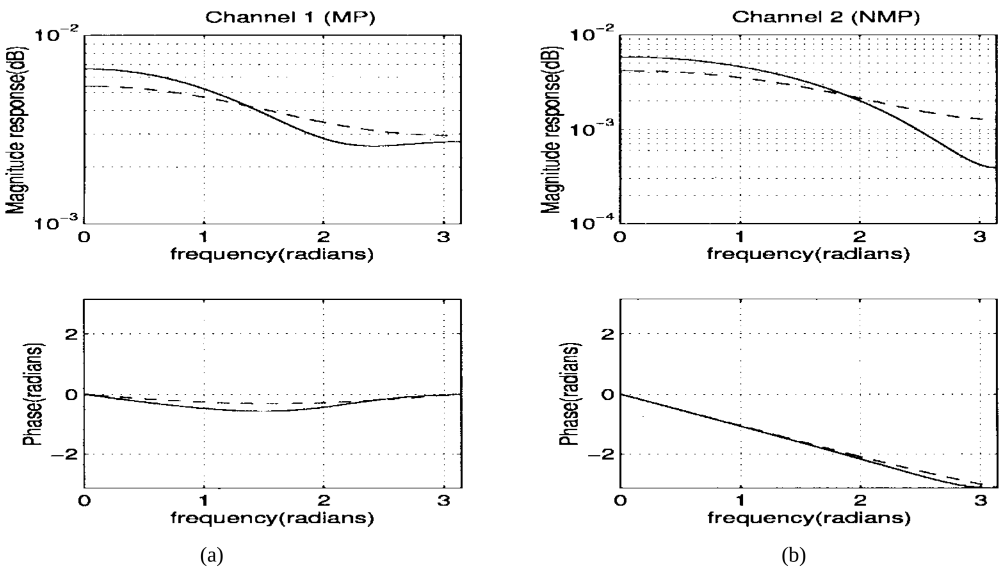

Fig. 2. Nonminimum-phase channel. Estimation via the trispectrum based scheme: $T = 4096$ samples. (a) Magnitude and phase of $H_{21}(\omega)$ (true: solid; estimated: dashed). (b) Magnitude and phase of $H_{12}(\omega)$ (true: solid; estimated: dashed). Input signals $s_1(t)$ and $s_2(t)$ are of equal strength.

Note that the cycle frequency α provides an additional degree of freedom that makes assumption **[C1′]** less severe than **[A1′]** and facilitates the simultaneous "diagonalization" of the fourth-order spectral matrix as described in Section III-A. That is, the procedure described in Section III-A for (non)stationary sources in effect operates only on the cyclic polyspectrum at $\alpha = 0$. While for a given cyclostationary source **[C1′]** may be violated for $\alpha = 0$, it is possible that it will hold true for other cycle frequencies α. The subsequent identification step for cyclostationary sources follows the algorithm described in Section III-B closely but with cyclic polyspectra instead of the conventional polyspectra.

VII. Simulations

The performance of the algorithms was tested with real speech signals and simulated data as well. After estimating $\mathbf{H}(\omega)$, the original signal was recovered via inverse filtering

$$\hat{\mathbf{s}}(\omega) = \hat{\mathbf{H}}^{-1}(\omega)\mathbf{x}(\omega). \tag{56}$$

The signal to interference ratio (SIR) at the input (before signal separation and as recorded by the sensors) and the output (after signal separation using the proposed algorithms) of the lth channel is defined as

$$\begin{aligned} \mathrm{SIR}_l^{\mathrm{IN}} &\triangleq 10\log_{10}\left[\frac{E\{s_l^2(t)\}}{E\{(x_l(t)-s_l(t))^2\}}\right] \\ \mathrm{SIR}_l^{\mathrm{OUT}} &\triangleq 10\log_{10}\left[\frac{E\{s_l^2(t)\}}{E\{(\hat{s}_l(t)-s_l(t))^2\}}\right]. \end{aligned} \tag{57}$$

A. Test Case 1

The trispectrum based algorithm was tested with channel impulse responses given by $h_{21} = [1,\ 0.5,\ 0.2]$ and $h_{12} = [0.3,\ 0.8,\ 0.4]$. The fourth-order cumulant lags $\hat{c}_{x_{l_0 l_1 l_2 l_3}}(\tau_1, \tau_2, \tau_3)$, $|\tau_i| \le 3$, $i = 1, 2, 3$ were estimated using $T = 4,096$ samples. The trispectrum was computed via the Fourier transform of the cumulant sequence. The input signals $s_1(t)$ and $s_2(t)$ were non-Gaussian AR with poles at -0.2 and -0.3, respectively. The true $\mathbf{H}(0)$ and the estimate resulting from the algorithm of Section III-A, were

$$\mathbf{H}(0) = \begin{bmatrix} 1 & 1.5 \\ 1.7 & 1 \end{bmatrix}, \quad \hat{\mathbf{H}}(0) = \begin{bmatrix} 1 & 1.46 \\ 1.37 & 1 \end{bmatrix}. \tag{58}$$

After extracting the system bispectra, the algorithm of [14] that performs log-magnitude reconstruction was employed to estimate $h_{12}(t)$ and $h_{21}(t)$. The mean (±std) of the channel impulse response estimates were $\hat{h}_{21} = [1.02(\pm 0.09),\ 0.32(\pm 0.09),\ 0.05(\pm 0.04)]$ and $\hat{h}_{12} = [0.17(\pm 0.15),\ 0.73(\pm 0.18),\ 0.24(\pm 0.16)]$ Fig. 2(a) and (b) shows the true and estimated transfer functions of the coupling systems (average of 100 trials). Note here that due to two stages of estimation, $\hat{h}_{12}(0) + \hat{h}_{12}(1) + \hat{h}_{12}(2) = 1.14 \ne \hat{H}_{12}(0)$ (similarly for the other channel). The input and output signal to interference ratios for $s_1(t)$ and $s_2(t)$

$$\mathrm{SIR}_1^{\mathrm{IN}} = 2.38 \text{ dB}, \quad \mathrm{SIR}_2^{\mathrm{IN}} = -0.29 \text{ dB}, \tag{59}$$

$$\mathrm{SIR}_1^{\mathrm{OUT}} = 11.20 \text{ dB}, \quad \mathrm{SIR}_2^{\mathrm{OUT}} = 10.31 \text{ dB} \tag{60}$$

also indicate good performance.

B. Test Case 2

Next the bispectrum-based algorithm was tested with $T = 512$ and 1024 data points. The input $s_1(t)$ was AR(1) with pole at -0.5 and $s_2(t)$ was AR(2) with poles at $-0.15 \pm j0.2784$. The channels were FIR with $h_{21} = [1,\ 0.5,\ 0.2]$, $h_{12} = [1,\ 0.2,\ -0.1]$. The variance ratio, $10\log[\mathrm{var}(s_1(t))/\mathrm{var}(s_2(t))]$ was -3 dB. The matrix $\mathbf{H}(0)$ was estimated first via the trispectrum-

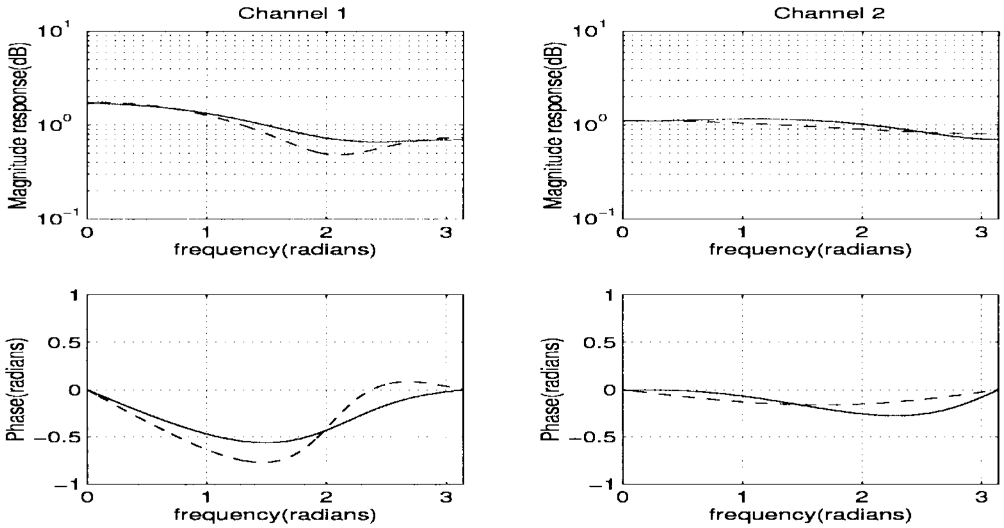

(a) (b)

Fig. 3. Estimation via the bispectrum based scheme: $T = 512$ samples. (a) Magnitude and phase of $H_{21}(\omega)$ (true: solid; estimated: dashed). (b) Magnitude and phase of $H_{12}(\omega)$ (true: solid; estimated: dashed). Input signals $s_1(t)$ and $s_2(t)$ are of equal strength.

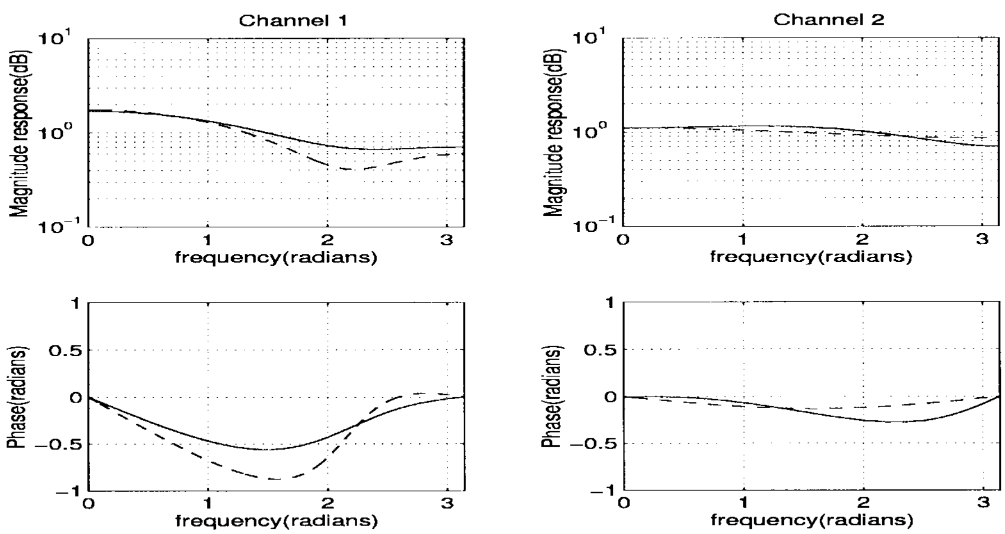

(a) (b)

Fig. 4. Estimation via the bispectrum based scheme: $T = 512$ samples. (a) Magnitude and phase of $H_{21}(\omega)$ (true: solid; estimated: dashed). (b) Magnitude and phase of $H_{12}(\omega)$ (true: solid; estimated: dashed). Signal $s_2(t)$ is twice as strong as $s_1(t)$.

based eigendecomposition scheme described in Section III-A. The bispectrum was computed via the bicorrelogram based method and eight lags were used. After extracting the system spectra (Section III-C), a spectral matching algorithm was employed to estimate the impulse responses. Fig. 4(a) and (b) shows the true and estimated frequency responses of the two channels (an average of 100 trials). The same experiment was repeated with $T = 1,024$ data points and the results are shown in Fig. 5(a) and (b). Performance is satisfactory in both cases, although because of unequal power signals, the estimator for h_{21} is worse than that of h_{12}. The SIR comparisons also indicated an improvement. The ratios with $s_1(t)$ and $s_2(t)$ as reference for $T = 512$ samples were

$$\mathrm{SIR}_1^{\mathrm{IN}} = -2.75 \text{ dB}, \quad \mathrm{SIR}_2^{\mathrm{IN}} = 3.83 \text{ dB}, \tag{61}$$

$$\mathrm{SIR}_1^{\mathrm{OUT}} = 7.58 \text{ dB}, \quad \mathrm{SIR}_2^{\mathrm{OUT}} = 11.95 \text{ dB}. \tag{62}$$

The ratios for $T = 1024$ showed a slight improvement over the corresponding ones for $T = 512$. In both cases, there was at least an 8 dB reduction in the interference even though the input signal levels were not the same. The corresponding mean ($\pm$ std) of the channel estimates for $T = 512$ were $\hat{h}_{21} = [0.84(\pm 0.26), 0.59(\pm 0.27), 0.35(\pm 0.34)]$, and $\hat{h}_{12} = [0.98(\pm 0.029), 0.13(\pm 0.04), 0.007(\pm 0.012)]$. With $T = 1024$, the coefficient estimates, $\hat{h}_{21} = [0.86 (\pm 0.16), 0.56(\pm 0.18), 0.38(\pm 0.29)]$ and $\hat{h}_{12} = [0.98(\pm$

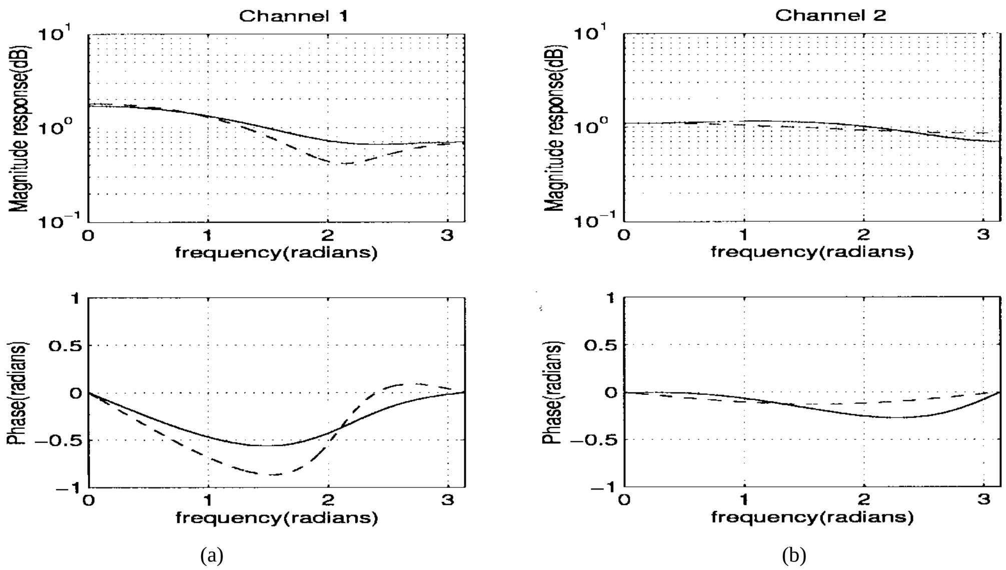

Fig. 5. Estimation via the bispectrum based scheme: $T = 1024$ samples. (a) Magnitude and phase of $H_{21}(\omega)$ (true: solid; estimated: dashed). (b) Magnitude and phase of $H_{12}(\omega)$ (true: solid; estimated: dashed). Signal $s_2(t)$ is twice as strong as $s_1(t)$.

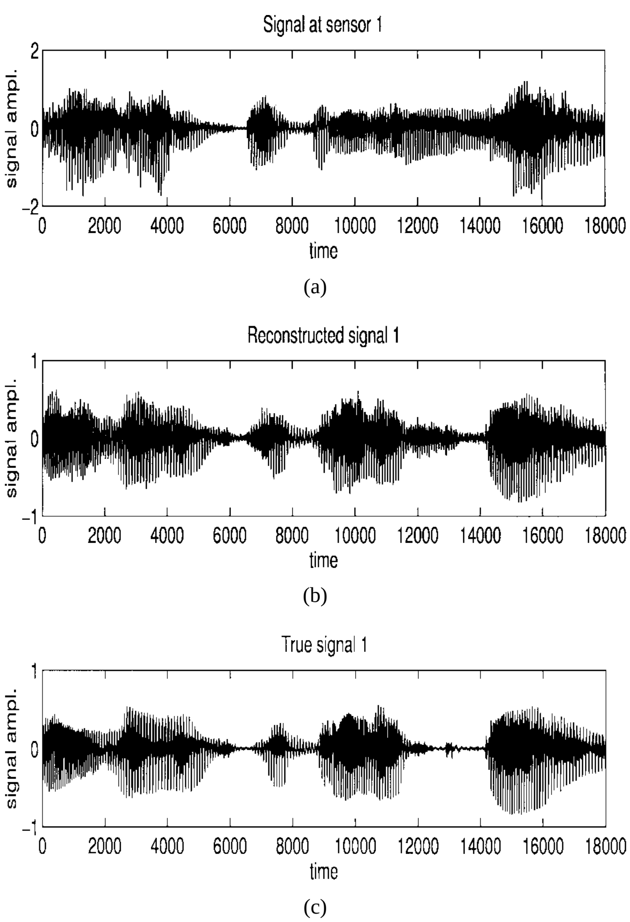

Fig. 6. $s_1(t)$: "He has the bluest eyes." Channel estimation using the proposed trispectrum based scheme: T =900 × 20 samples. (a) $x_1(t) = s_1(t)+$ interf. (b) $\hat{s}_1(t)$: reconstructed. (c) $s_1(t)$: true.

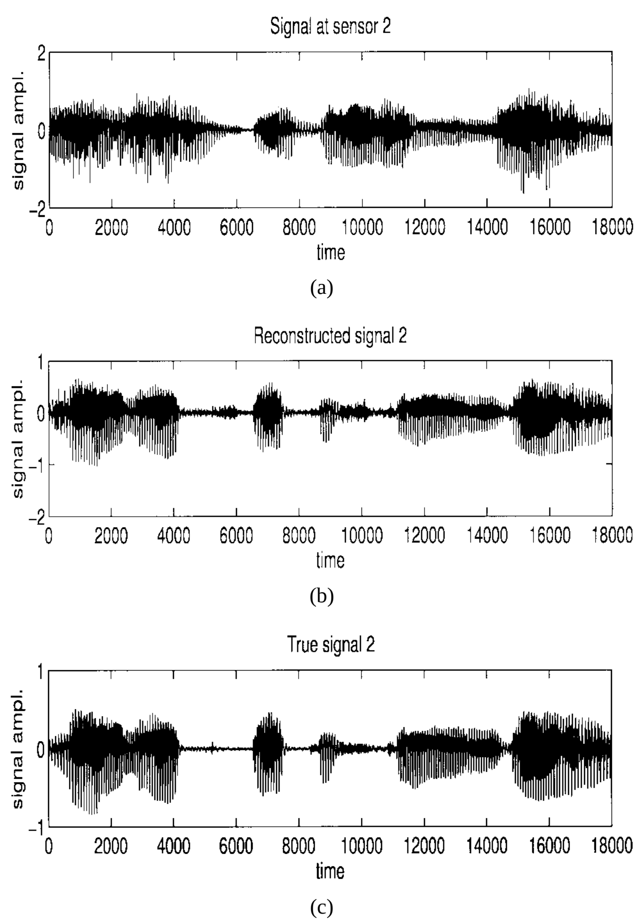

Fig. 7. $s_2(t)$: "Line up at the screen door." Channel estimation using the proposed trispectrum based scheme: T =900 × 20 samples. (a) $x_2(t) = s_2(t)+$ interf. (b) $\hat{s}_2(t)$: reconstructed. (c) $s_2(t)$: true.

$0.02), 0.13(\pm 0.02), 0.005(\pm 0.007)]$ show lower bias and variance when compared with those obtained with $T = 512$.

For comparison, the results under the condition $\text{var}(s_1(t)) = \text{var}(s_2(t)) = 1$ are shown in Fig. 3. The performance is clearly better in this case even with $T = 512$ data points and the

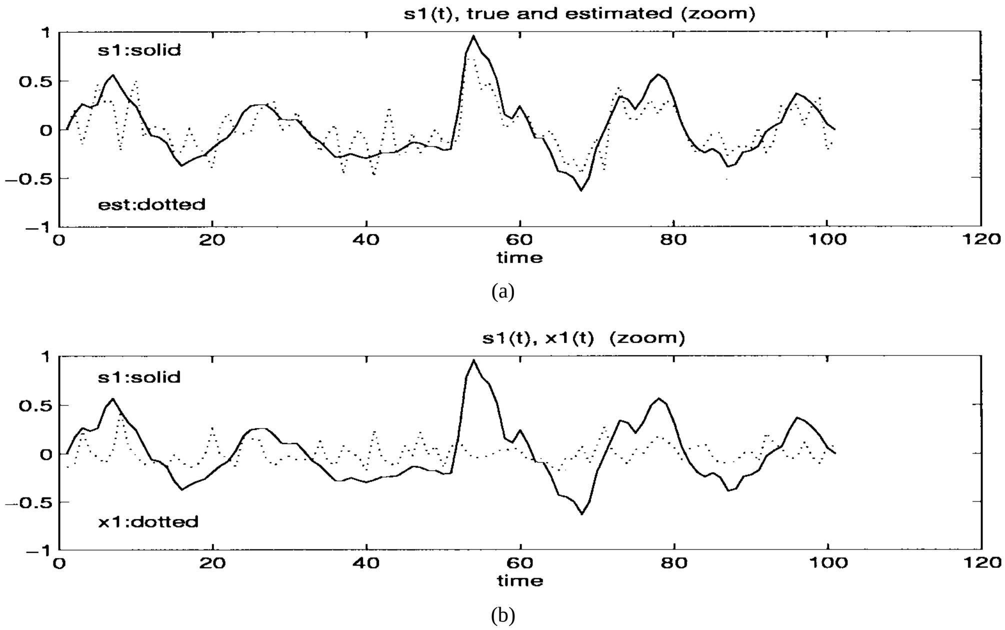

Fig. 8. $s_1(t)$ is a segment of phoneme /*ae*/. Channel estimation using the proposed bispectrum based scheme: $T = 1200$ samples. (a) $s_1(t)$: solid; $\hat{s}_1(t)$: dotted. (b) $s_1(t)$: solid; $x_1(t) = s_1(t)+$ interf.: dotted.

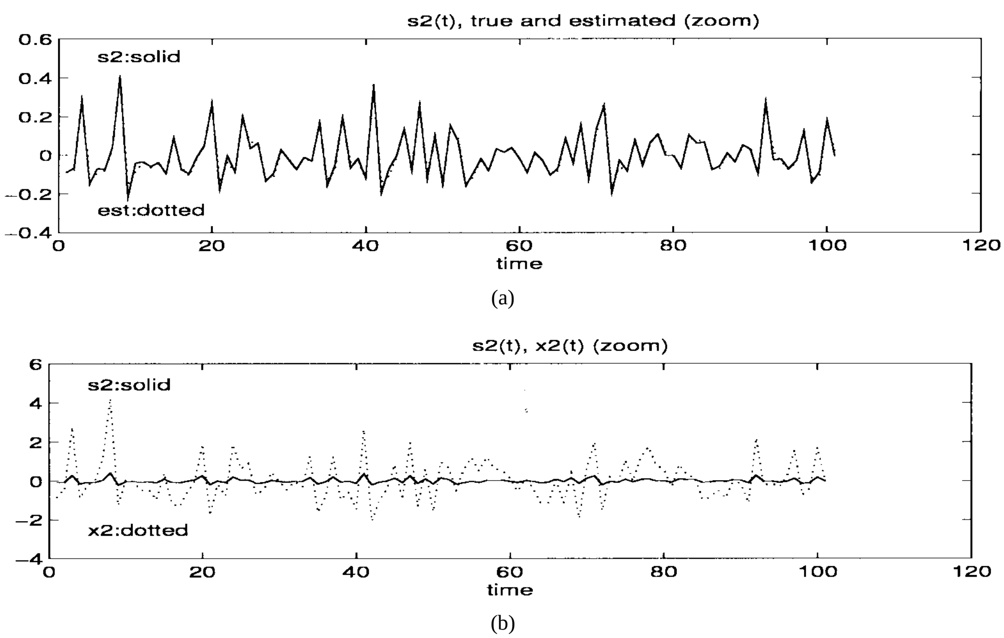

Fig. 9. $s_2(t)$ is an AR(3) non-Gaussian process. Channel estimation using the proposed bispectrum-based scheme: $T = 1200$ samples. (a) $s_2(t)$: solid; $\hat{s}_2(t)$: dotted. (b) $s_2(t)$: solid; $x_1(t) = s_2(t)+$ interf.: dotted.

variance of $\hat{h}_{12}$ is slightly lower when compared to the unequal power case. The interference was reduced by about 11 dB in both channels as a result of the proposed processing scheme. The corresponding mean (±std) of the channel estimates were $\hat{h}_{21} = [0.90(\pm 0.24),\ 0.52(\pm 0.19),\ 0.36(\pm 0.39)]$ and $\hat{h}_{12} = [0.96(\pm 0.04),\ 0.16(\pm 0.06),\ 0.005(\pm 0.017)]$.

C. Test Case 3

The proposed trispectrum-based channel estimation and signal reconstruction scheme was also tested on the speech data used in [20]. The channel impulse responses were $h_{21} = [0.8,\ 0.5,\ 0.2]$ and $h_{12} = [1,\ 0.6,\ 0.3]$. The signals $s_1(t)$ and $s_2(t)$ were speech signals corresponding to the sentences, "He has the bluest eyes," and "Line up at the screen door." The outputs $x_1(t)$ and $x_2(t)$ were generated according to (1), and $T = 18\,000$ samples were used. The trispectrum was estimated via the sample cumulant as in Test Case 1 but the estimation was performed using smaller segments of length $L = 900$. For each segment, the channel bispectra were extracted from the trispectra of $x_1(t)$ and $x_2(t)$ as described in Section III. The magnitude and phase of $H_{12}(\omega)$ and $H_{21}(\omega)$ was estimated via the linear algorithm of [14]. Finally, the input signals were recovered via inverse filtering. Fig. 6 shows $x_1(t)$, the signal recorded by sensor 1, the estimated and true input signal $s_1(t)$. The corresponding signals for the other channel are shown in Fig. 7. Note that while $x_1(t)$ and $x_2(t)$ look very similar, the recovered signals compare favorably with the original sentences. The SIR ratios before and after processing also show improvement, as follows:

$$\mathrm{SIR}_1^{\mathrm{IN}} = -4.25 \text{ dB}, \quad \mathrm{SIR}_2^{\mathrm{IN}} = -4.23 \text{ dB}, \qquad (63)$$
$$\mathrm{SIR}_1^{\mathrm{OUT}} = 8.65 \text{ dB}, \quad \mathrm{SIR}_2^{\mathrm{OUT}} = 7.51 \text{ dB}. \qquad (64)$$

D. Test Case 4

This example demonstrates the applicability of the proposed procedure to a mixture of nonstationary and stationary signals. The desired signal was the phoneme /*ae*/ uttered by a female speaker. The second signal was an AR(3) non-Gaussian process with poles at $-0.0545 \pm 0.4915j$ and -0.4089. The time-averaged bispectrum was computed using $T = 1200$ data points. The impulse response was estimated via spectral matching after extracting the channel spectra via the algorithm of Section III-C. Figs. 8 and 9 show the true, corrupted, and estimated signals at channels one and two, respectively. In Fig. 8(a), we note that the reconstructed signal has little residual interference ($\mathrm{SIR}_1^{\mathrm{IN}} = 0.33$ dB, $\mathrm{SIR}_1^{\mathrm{OUT}} = 3.98$ dB). The signal to interference levels for $s_2(t)$ ($\mathrm{SIR}_2^{\mathrm{IN}} = -18.5$ dB, $\mathrm{SIR}_2^{\mathrm{OUT}} = 16.02$ dB) also shows significant improvement [see Fig. 9(a) and (b)]. The separation was successful and the performance is reasonably good with estimation using a single record.

VIII. Conclusion

By exploiting cross-polyspectra between channel outputs, input signal and channel estimation methods were proposed. By exploiting the structure of a special multichannel model that shows up in a variety of applications, unique extraction of (possibly colored) input signals was achieved. The resulting linear algorithms yield the true inputs if the channels are FIR and leave a shaping filter ambiguity in all other cases. An alternate approach to resolve the shaping filter ambiguity is to use the ideas underlying parameter pairing in two-dimensional ESPRIT. This would increase the computational complexity of the algorithm, but would lead to a closed-form solution to the shaping filter identification.

By employing time-averaged polyspectra, the methods are also useful when a mixture of stationary and quasiperiodic (cyclostationary) signals are involved. Currently, the performance of the proposed algorithms and extensions to time-varying channels is being explored.

References

[1] D. R. Brillinger, *Time Series: Data Analysis and Theory*. San Francisco, CA: Holden Day, 1981.

[2] D. R. Brillinger and M. Rosenblatt, "Computation and interpretation of kth-order spectra," *Spectral Analysis of Time-Series*, B. Harris, Ed. New York: Wiley, 1967, pp. 189–232.

[3] V. Capdevielle, C. Serviere, and J. L. Lacoume, "Separation of wideband sources," in *Proc. IEEE Workshop Higher-Order Statistics*, Barcelona, Spain, June 1995, pp. 66–70.

[4] J.-F. Cardoso, "Source separation using higher-order moments," in *Proc. ICASSP*, Glasgow, U.K., 1989, vol. 4, pp. 2109–2112.

[5] J.-F. Cardoso and A. Souloumiac, "Blind beamforming for non-Gaussian signals," in *Proc. Inst. Electr. Eng. Ser. F*, vol. 140, pp. 362–370, Dec. 1993.

[6] P. Comon, "Separation of stochastic processes," in *Proc. Workshop Higher-Order Spectral Analysis*, Vail, CO, July 1989, pp. 174–179.

[7] P. Comon, "MA estimation using fourth-order cumulants," *Signal Process.*, vol. 26, pp. 381–388, Mar. 1992.

[8] ——, "Independent component analysis: A new concept?" *Signal Process.*, vol. 36, pp. 287–314, Apr. 1994.

[9] A. V. Dandawate and G. B. Giannakis, "Nonparametric polyspectral estimators for kth-order (almost) cyclostationary processes," *IEEE Trans. Inform. Theory*, vol. 40, pp. 67–84, Jan. 1994.

[10] A. V. Dandawate and G. B. Giannakis, "Asymptotic theory of mixed time averages and kth-order cyclic- moment and cumulant statistics," *IEEE Trans. Inform. Theory*, vol. 41, pp. 216–232, Jan. 1995.

[11] G. B. Giannakis, Y. Inouye, and J. M. Mendel, "Cumulant-based parameter estimation of multichannel moving-average processes," *IEEE Trans. Automat. Contr.*, pp. 783–787, July 1989.

[12] M. Najar, M. Lagunas, and I. Bonet, "Blind wideband source separation," in *Proc. ICASSP*, Apr. 1994, vol. IV, pp. 65–68.

[13] B. Porat, *Digital Processing of Random Signals*. Englewood Cliffs, NJ: Prentice-Hall, 1993.

[14] M. Rangoussi and G. B. Giannakis, "FIR modeling using log-bispectra: Weighted least-squares algorithms and performance analysis," *IEEE Trans. Circuits Syst.*, pp. 281–296, 1991.

[15] S. Shamsunder and G. B. Giannakis, "Wideband source modeling and localization: A HOS based approach," in *Proc. 25th Asilomar Conf. Signals, Systems, and Computers*, Pacific Grove, CA, Nov. 1991, pp. 383–387.

[16] ——, "Modeling of non-Gaussian array data using cumulants: DOA estimation of more sources with less sensors," *Signal Process.*, vol. 30, pp. 279–298, Feb. 1993.

[17] A. Swami, G. B. Giannakis, and S. Shamsunder, "Multichannel ARMA processes," *IEEE Trans. Signal Processing*, vol. 42, pp. 898–913, Apr. 1994.

[18] L. Tong, R. Liu, V. C. Soon, and Y.-F. Huang, "Indeterminacy and identifiability of blind identification," *IEEE Trans. Circuits Syst.*, pp. 499–509, May 1991.

[19] L. Tong, Y. Inouye, and R. Liu, "Waveform preserving blind estimation of multiple independent sources," *IEEE Trans. Signal Processing*, vol. 41, pp. 2461–2470, July 1993.

[20] E. Weinstein, M. Feder, and A. V. Oppenheim, "Multi-channel signal separation by decorrelation," *IEEE Trans. Speech Audio Processing*, vol. 1, pp. 405–413, Oct. 1993.

[21] B. Widrow *et al.*, "Adaptive noise canceling: Principles and application," in *Proc. IEEE*, pp. 1692–1716, 1975.

[22] D. Yellin and E. Weinstein, "Criteria for multi-channel signal separation," *IEEE Trans. Signal Processing*, vol. 42, pp. 2158–2168, Aug. 1994.

Sanyogita Shamsunder received the Bachelor's degree in electronics and communication engineering from Osmania University, Hyderabad, India, in 1987, and the M.S. degree in 1989 from the State University of New York, Stony Brook, and the Ph.D. degree, in 1994, from the University of Virginia, Charlottesville, both in electrical engineering.

She has been an Assistant Professor with the Department of Electrical Engineering, Colorado State University, Fort Collins, since 1994. Her current research interests lie in the area of statistical signal processing, estimation, and detection. Particular applications include antenna array and multichannel signal processing, underwater acoustics, and telecommunications and speech.

Dr. Shamsunder has been on the editorial board of the IEEE Signal Processing Magazine since 1994. She is a member of, and faculty advisor for, Eta Kappa Nu.

Georgios B. Giannakis (F'96) received the Dipl. degree in electrical engineering from the National Technical University of Athens, Greece, in 1981. He received the M.Sc. degree in electrical engineering in 1983, the M.Sc. degree in mathematics, in 1986, and the Ph.D. degree in electrical engineering in 1986, all from the University of Southern California (USC), Los Angeles.

After lecturing for one year at USC, he joined the University of Virginia, Charlottesville, in September 1987, where he is now a Professor with the Department of Electrical Engineering. His general interests lie in the areas of signal processing, estimation and detection theory, and system identification. Specific research areas of current interest include diversity techniques for channel estimation and multiuser communications, nonstationary and cyclostationary signal analysis, wavelets in statistical signal processing, and non-Gaussian signal processing with applications to SAR, array and image processing.

Dr. Giannakis received the IEEE Signal Processing Society's 1992 Paper Award in the Statistical Signal and Array Processing area. He co-organized the 1993 IEEE Signal Processing Workshop on Higher Order Statistics, the 1996 IEEE Workshop on Statistical Signal and Array Processing, and the first IEEE Signal Processing Workshop on Wireless Communications in 1997. He guest co-edited the special issues on high-order statistics of *International Journal of Adaptive Control and Signal Processing* and the EURASIP journal *Signal Processing*, and the January 1997 special issue of the IEEE TRANSACTIONS ON SIGNAL PROCESSING on signal processing for advanced communications. He has served as an Associate Editor for the IEEE TRANSACTIONS ON SIGNAL PROCESSING and the IEEE SIGNAL PROCESSING LETTERS. He has been a secretary of the Signal Processing Conference Board, and is a member of the SP Publications board and the SSAP Technical Committee. He is also a member of the IMS and the European Association for Signal Processing.